비선형 최소 자승법을 이용한 이동 로봇의 비주얼 서보 네비게이션

Visual Servo Navigation of a Mobile Robot Using Nonlinear Least Squares Optimization for Large Residual

김 곤 우[1], 남 경 태[1], 이 상 무[1], 손 웅 희[2]

Gon-Woo Kim[1], Kyung-Tae Nam[1], Sang-Moo Lee[1], Woong-Hee Shon[2]

Abstract We propose a navigation algorithm using image-based visual servoing utilizing a fixed camera. We define the mobile robot navigation problem as an unconstrained optimization problem to minimize the image error between the goal position and the position of a mobile robot. The residual function which is the image error between the position of a mobile robot and the goal position is generally large for this navigation problem. So, this navigation problem can be considered as the nonlinear least squares problem for the large residual case. For large residual, we propose a method to find the second-order term using the secant approximation method. The performance was evaluated using the simulation.

Keywords : Visual servoing, Image Jacobian, Navigation, Unconstrained optimization, Nonlinear least squares

1. Introduction

Visual feedback control is generally referred to as visual servoing which is control method using visual information[1]. The image-based visual servoing is visual feedback control to use the image error directly to control the robot with the image Jacobian.

Many researchers have proposed visual servoing algorithm for robotic manipulators[2][3][5]. For visual servoing of mobile robots, many researchers have been focused on on-board camera[7][8][9][10]. Midorikawa et al. in [7] incorporated virtual image plane acquired by sensor fusion of vision and encoder in the proposed assist mobile robot system. Zhang et al. in [11] proposed a visual motion planning algorithm which can make motion plans directly in the image plane. For eye-to-hand configuration, Dixon et al. in [6] proposed an asymptotic pose tracking controller which is developed for a wheeled mobile robot with an uncalibrated ceiling mounted camera system.

In this paper, the composite image Jacobian is proposed using the kinematic model of a wheeled mobile robot and the perspective transformation[6]. This composite image Jacobian can be efficiently used for image-based visual servoing of a wheeled mobile robot. We also define the mobile robot navigation problem as an unconstrained optimization problem to minimize the image error between the goal position and the position of a mobile robot in the image plane. Nonlinear least squares algorithm has been adopted for solving this unconstrained optimization problem. The residual function which is the image error between the position of a mobile robot and the goal position is generally large for this navigation problem. For large residual, we propose an efficient method to find the second-order term using the secant approximation method.

The paper is organized as follows. In section 2,

※ 본 연구는 산업자원부 지원으로 수행하는 차세대 성장동력 기술개발 사업의 일환으로 수행되었음

[1] 한국생산기술연구원 로봇기술본부 선임연구원
(E-mail : kgw0510@kitech.re.kr, robotnam@kitech.re.kr, lsm@kitech.re.kr)

[2] 한국생산기술연구원 로봇기술본부 수석 연구원
(E-mail : shon@kitech.re.kr)

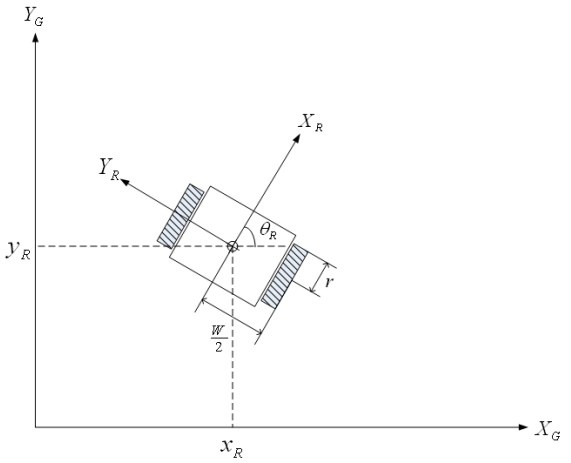

Fig.1. Definition of coordinate systems: the global reference frame, {G}, the robot reference frame, {R}

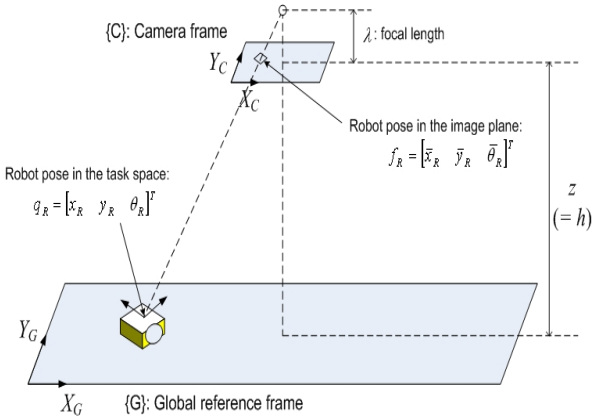

Fig.2. Configuration of robot and camera system

visual servoing for mobile robot navigation is presented. Perspective transformation is also addressed for the task space to the image plane. Section 3 presents image-based visual servo navigation using nonlinear least squares optimization method for large residual. In order to evaluate the proposed visual servoing, some simulation results are shown in Section 4. Finally, brief conclusions are presented in Section 5.

2. Visual Servoing for Mobile Robot Navigation

2.1 Kinematics for Differential Drive Robot System

Kinematics is the most basic study about mechanical behavior of robot system. Relative position of mobile robots can be estimated using kinematic models.

Kinematics for mobile robots is somewhat different from robot manipulators. Robot manipulators can be considered to be more complex than mobile robot in some way because standard robot manipulators generally have six or more joints, whereas differential drive robots have only two wheels. A robot manipulator is fixed to the environment; therefore the pose of its end effector can be achieved by the relation between its end effector and its fixture. However, a mobile robot is not fixed to the environment; therefore its pose can be achieved in its environment.

The major difference between a mobile robot and a robot manipulator is the method of position estimation. For the case of a robot manipulator, the pose of its end effector can be measured by the kinematics of the robot and the position of all intermediate joints. When we know the position of all joints, the pose of the robot end effector is always measurable. However, we cannot directly measure the pose of a mobile robot instantaneously because a mobile robot can move by itself in its environment.

The pose of a mobile robot in the global reference frame can be defined as shown in Fig. 1 and Fig. 2 as:

$$q_R = [x_R \quad y_R \quad \theta_R]^T \tag{1}$$

where x_R, y_R, and θ_R denote the position and orientation of a mobile robot, respectively.

The kinematic model of a differential drive robot with wheel diameter r is shown by using Jacobian matrix as[6][7]:

$$\dot{q}_R = J_{kin} \cdot \dot{\varphi}$$
$$where \quad J_{kin} = \begin{bmatrix} r\cos\theta_R/2 & r\cos\theta_R/2 \\ r\sin\theta_R/2 & r\sin\theta_R/2 \\ r/W & r/W \end{bmatrix} \tag{2}$$

where $\dot{\varphi}$ is the rotating speed of each wheel, $\dot{\varphi}_r$ and $\dot{\varphi}_l$ and W is the distance between two wheels.

Using the linear and angular velocity of a mobile robot, the speed of a mobile robot can be acquired as:

$$\dot{q}_R = T(q_R) \cdot \begin{bmatrix} v_R \\ \omega_R \end{bmatrix} \quad where \quad T(q_R) = \begin{bmatrix} \cos\theta_R & 0 \\ \sin\theta_R & 0 \\ 0 & 1 \end{bmatrix} \tag{3}$$

where v_R and ω_R are the linear and angular velocity of a mobile robot, respectively.

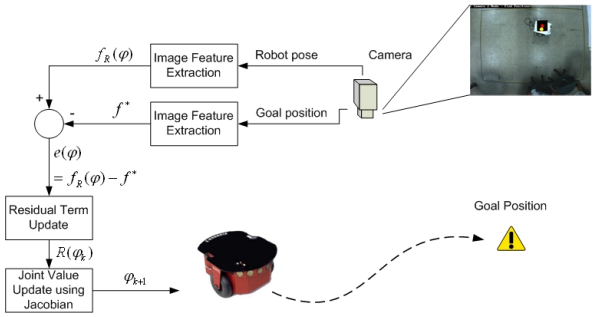

Fig.3 The control architecture of the proposed image-based visual servo control system

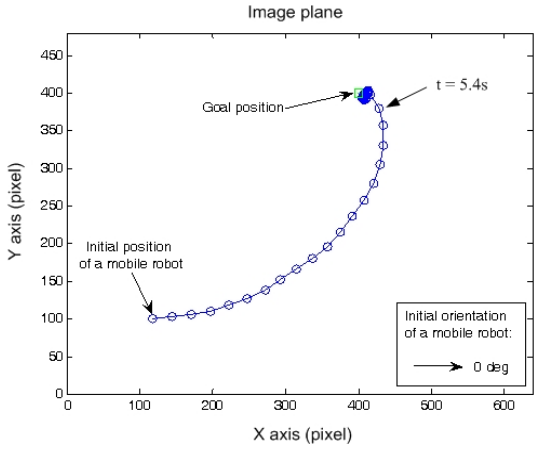

(a)

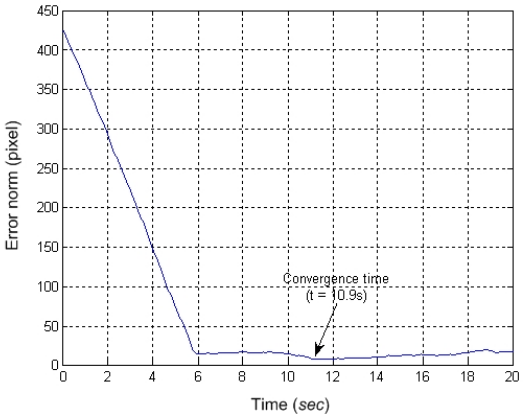

(b)

Fig.4 The simulation results for the zero residual case (R(φk)=0) when the robot pose is [100 100 0°]T: (a) the trajectory of a mobile robot, and (b) the pixel error norm

2.2 Perspective Transformation for the Task Space to the Image Plane

The kinematic model in the image plane can be

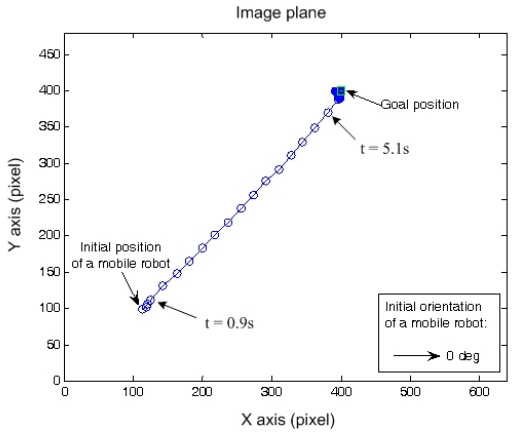

(a)

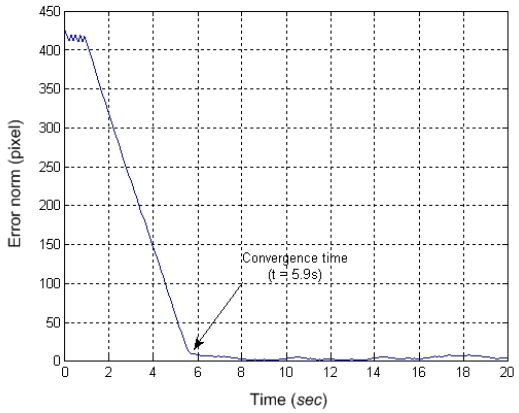

(b)

Fig.5. The simulation results for the large residual case (R(φk)≠0) when the robot pose is [100 100 0°]T: (a) the trajectory of a mobile robot, and (b) the pixel error norm

modeled using the similar manner in the previous section. The pose of a mobile robot in the image plane as shown in Fig. 2 can be defined as:

$$f_R = \begin{bmatrix} \bar{x}_R & \bar{y}_R & \bar{\theta}_R \end{bmatrix}^T \tag{4}$$

where $\bar{x}_R$, $\bar{y}_R$, and $\bar{\theta}_R$ denote the position and orientation of a mobile robot in the image plane, respectively.

The configuration of robot and camera system is shown in Fig. 2. The camera is fixed on the ceiling and its image plane is assumed to be parallel to the plane of the robot workspace. And we assume that the origin and the axes in the task space correspond to the origin and the axes in the image plane.

The kinematic model of a mobile robot in the image plane is shown by using the linear and angular velocity in the image plane as:

$$\dot{f}_R = \bar{T}(f_R)\cdot\begin{bmatrix}\bar{v}_R\\ \bar{\omega}_R\end{bmatrix} \quad where \quad \bar{T}(f_R)=\begin{bmatrix}\cos\bar{\theta}_R & 0\\ \sin\bar{\theta}_R & 0\\ 0 & 1\end{bmatrix} \tag{5}$$

where $\bar{v}_R$ and $\bar{\omega}_R$ are the linear and angular velocity of a mobile robot in the image plane, respectively.

In order to find the position and orientation of a robot in the image plane, we know the relationship between the position in the task space and the position in the image plane. The position of a robot in the image plane can be acquired using the position of a robot in the task space by the perspective transformation which projects 3-D points onto a plane as:

$$\begin{bmatrix}\bar{x}_R\\ \bar{y}_R\end{bmatrix}=\frac{\lambda}{h}\begin{bmatrix}k_u & 0\\ 0 & k_v\end{bmatrix}\begin{bmatrix}x_R\\ y_R\end{bmatrix} \tag{6}$$

where λ is the focal length of the camera and k_u, k_v are the conversion parameters (unit: pixel/m) to convert the unit of the task space to the pixel level in the image plane.

We can find the Jacobian matrix which represents the relationship between the linear and angular velocity in the task space and the linear and angular velocity in the image space as follows:

$$\begin{bmatrix}v_R\\ \omega_R\end{bmatrix}=J_{img}\cdot\begin{bmatrix}\bar{v}_R\\ \bar{\omega}_R\end{bmatrix}=\begin{bmatrix}J_1 & 0\\ 0 & J_2\end{bmatrix}\cdot\begin{bmatrix}\bar{v}_R\\ \bar{\omega}_R\end{bmatrix}$$
$$where \quad J_1=\frac{1}{\alpha}\cos\bar{\theta}_R\cos\theta_R+\frac{1}{\beta}\sin\bar{\theta}_R\sin\theta_R \tag{7}$$
$$J_2=\frac{\alpha}{\beta}\cos^2\theta_R+\frac{\beta}{\alpha}\sin^2\theta_R$$

where α and β are $\lambda\cdot k_u/h$ and $\lambda\cdot k_v/h$, respectively[6].

The final goal of this section is to find the composite image Jacobian which represents the relationship between the speed of wheels of a mobile robot and the robot's overall speed in the image plane. A mobile robot can be directly controlled in the image plane using the composite image Jacobian, which is called the image-based visual servo control.

The composite image Jacobian, $J_\varphi \in R^{3\times 2}$, can be acquired as:

$$\dot{f}_R=\bar{T}(f_R)\cdot J_{img}^{-1}\cdot T^{+}(q_R)\cdot J_{kin}\cdot\dot{\varphi}=J_\varphi\cdot\dot{\varphi} \tag{8}$$

where $T^{+}(q_R)$ is the pseudo inverse matrix of $T(q_R)$ as $T^{+}(q_R)=(T^T\cdot T)^{-1}\cdot T^T$.

The rotational speed of wheels of a mobile robot can be directly related to the overall speed of a mobile robot in the image plane using the composite image Jacobian in (8).

3. Nonlinear Least Squares Optimization for Mobile Robot Navigation

We define the visual servo navigation of a mobile robot as the unconstrained optimization problem to move a mobile robot to a goal position. The nonlinear least squares optimization method is used for solving this problem. Fig. 3 shows the control architecture of the image-based visual servo control system.

3.1 Cost Function for Visual Servo Navigation

Considering the eye-to-hand vision system, the camera can observe the pose of the mobile robot in the image plane as shown in Fig. 3. In the image plane, the goal position is virtually represented by f^* and the pose of the mobile robot is represented by $f_R(\varphi)$ as the function of the robot wheel variables, φ. The control problem which is to move a mobile robot to a goal position can be defined as the minimization of the image error.

In order to minimize the image error between the goal position and the pose of the mobile robot, we define the cost function as:

$$E(\varphi)=\frac{1}{2}e(\varphi)^T e(\varphi) \quad where \; e(\varphi)=f_R(\varphi)-f^* \tag{9}$$

which is defined by the square of the image error. This cost function is a nonlinear function because the image feature of a mobile robot is determined by the complex geometric relationship.

3.2 Full Newton's Method for Nonlinear Least Squares Optimization

The nonlinear least squares optimization problem for moving a mobile robot toward a goal position can be defined as:

$$\min_{\varphi \in R^n} E(\varphi) = \min_{\varphi \in R^n} \frac{1}{2} e(\varphi)^T e(\varphi) \tag{10}$$

which is minimized at the robot joint configuration, φ^*, satisfying the equation, $\partial E(\varphi^*)/\partial\varphi=0$. If we assume the linear model in the neighborhood at $\bar{\varphi}$, the cost function can be approximated using the Taylor series expansion as:

$$\hat{E}(\varphi) = E(\bar{\varphi}) + \nabla E(\bar{\varphi}) \cdot (\varphi - \bar{\varphi}) \tag{11}$$

If we assume that the cost function is the second order differentiable for φ, the gradient of the approximation model is shown as:

$$\frac{\partial \hat{E}(\varphi)}{\partial \varphi} = \nabla E(\bar{\varphi}) + \nabla^2 E(\bar{\varphi}) \cdot (\varphi - \bar{\varphi}) \tag{12}$$

We define the composite image Jacobian of robot, $J_\varphi(\varphi)= \partial f_R(\varphi)/\partial\varphi$, in (8). The cost function can be the minimizer of the cost function if the gradient of the approximation model at φ_k is zero. The iterative form of the joint value to minimize the cost function becomes:

$$\varphi_{k+1} = \varphi_k - \left(J_\varphi(\varphi_k)^T J_\varphi(\varphi_k) + R(\varphi_k)\right)^{-1} J_\varphi(\varphi_k)^T e(\varphi_k) \tag{13}$$

where the residual term, $R(\varphi)$ is $R(\varphi) = \nabla\left(J_\varphi(\varphi)\right)^T e(\varphi)$.

3.3 Finding Residual Term using Secant Approximation Method for Large Residual

The residual function which is the image error between the position of a mobile robot and the goal position is generally large for this navigation problem. So, this navigation problem can be considered as the large residual case for nonlinear least squares problem.

The term, $R(\varphi)$, in (13) is difficult to compute analytically because it contains the Hessian term of the image error. Therefore, this term has been commonly ignored in some researches[2]. We propose the method to estimate the residual term for more precise modeling using the secant approximation method.

We have to compute the Hessian matrix of the robot feature vector, $\nabla^2 f_R(\varphi)$, in order to find the gradient of the composite image Jacobian of a mobile robot. Using the secant approximation method, the iterative form of $R(\varphi)$ at φ_k can be calculated as follows:

$$R(\varphi_k) = \frac{\left(J_\varphi(\varphi_k) - J_\varphi(\varphi_{k-1})\right)^T e(\varphi_k)(\varphi_k - \varphi_{k-1})^T}{(\varphi_k - \varphi_{k-1})^T(\varphi_k - \varphi_{k-1})} \tag{14}$$

4. Performance Analysis of Visual Servo Navigation

The proposed methods were applied on a differential drive mobile robot for the eye-to-hand configuration. The simulation was performed for the algorithm to find the term, R(φ), for the large residual case and the results were compared with the results for the zero residual case.

A mobile robot is nonholonomic system. Therefore, performance of navigation is greatly affected by the orientation data of a mobile robot at the initial position. Therefore, the simulation was performed for different orientations at the same position of a mobile robot.

The initial position of a mobile robot is (100, 100) and the goal position is (400, 400) in the image plane. The sampling time is 100 ms. The steady-state is defined as the state after achieving $\|e(\varphi_k)\|_2 \leq$ 10 pixels. In this simulation, the observation noise was added for the robot pose in (4). The variance of the observation noise was set to (2 pixels, 2 pixels, 0.1°).

Fig. 4 and Fig. 5 present the results for both the zero residual case and the large residual case when the initial pose of a mobile robot is $[100\ 100\ 0°]^T$, respectively. For the zero residual case, the average steady-state error norm in pixel is 12.0776 pixels and the convergence time is 10.9 sec as shown in Fig. 4 (a). For the large residual case, however, the average steady-state error norm in pixel is 3.407 pixels and the convergence time is 5.9 sec as shown in Fig. 5 (a). The trajectory of a mobile robot for both cases is shown in Fig. 4 (b) and Fig. 5 (b). The heading direction for the

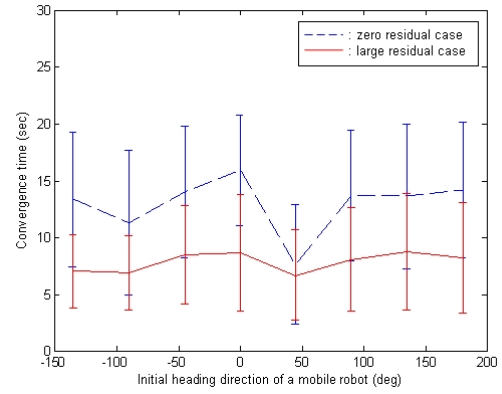

(a)

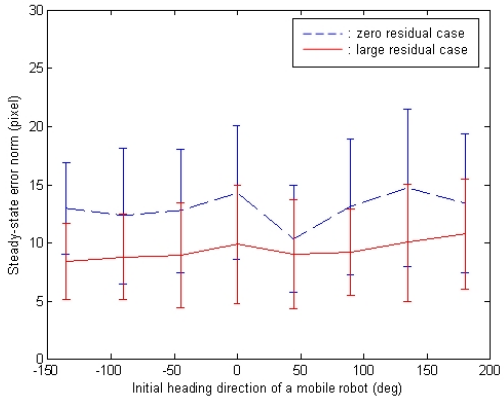

(b)

Fig.6. The comparison of the results for the zero residual case and for the large residual case according to the different orientation of a mobile robot: (a) the convergence time, and (b) the average steady-state error

large residual case has been adjusted faster than the heading direction for the zero residual case toward the goal position (about 45°) as shown in Fig. 4 (b) and Fig. 5 (b). This is one reason of fast convergence time and small steady-state error for the large residual case.

According to the simulation, the results for the large residual case show better performance than the results for the zero residual case. The simulation performed 100 iterations under the same condition for each orientation. Fig. 6 shows the results of the convergence time and the average steady-state error for the zero residual case and the large residual case. The mean and the standard deviation of the convergence time have been acquired through 100 iterations for each orientation. These results are plotted in Fig. 6. The convergence time for the large residual case is shorter than the convergence time for the zero residual case as shown in Fig. 6 (a). However, the results of the convergence time for both cases are almost similar when the initial heading direction of a mobile robot is 45°. For the average steady-state error, the results for both cases are also similar when the initial heading direction of a mobile robot is 45° as shown in Fig. 6 (b). Except these results, the average steady-state error for the large residual case is smaller than the average steady-state error for the zero residual case. When the initial heading direction of a mobile robot is 45°, the orientation term of the image error is nearly zero. Through the results, we can see that the term, $R(\varphi)$, affects the orientation of a mobile robot. The composite image Jacobian in (8) has only the information of the position error. However, the term, $R(\varphi)$, includes the information of the position and orientation error. Therefore, the term, $R(\varphi)$, dominantly affects the fast convergence of the orientation error in (13).

5. Conclusions

We propose a navigation algorithm using image-based visual servoing utilizing a fixed camera. Nonlinear least squares algorithm was adopted for solving the unconstrained optimization problem. The composite image Jacobian was applied to nonlinear least squares algorithm. For large residual, an efficient method was also proposed using the secant approximation method in order to find the second-order term. The simulation results showed the validity of the proposed image-based visual servoing algorithm.

References

[1] S. Hutchison, G. D. Hager, and P. I. Corke, “A Tutorial on visual servo control,” IEEE Trans. Robotics and Automation, vol. 12, no. 5, Oct. 1996, pp. 651-670.

[2] J. A. Piepmeier, G. V. McMurray, and H. Lipkin, “A dynamic quasi-Newton method for uncalibrated visual servoing,” IEEE Int'l Conf. Robotics and Automation, 1999, pp. 1595-1600.

[3] G. W. Kim, B. H. Lee, and M. S. Kim, “Uncalibrated visual servoing technique using large residual,” IEEE Int'l Conf. Robotics and Automation, 2003, pp. 3315-3320.

[4] F. Conticelli, B. Allotta, and P. K. Khosla, “Image-Based Visual Servoing of Nonholonomic Mobile Robots,” Int'l Conf. Decision and Control, 1999, pp. 3496-3501.
[5] G. W. Kim, and B. H. Lee, “Target Tracking using the Efficient Estimation of the Image Jacobian with Large Residual,” ROBOTICA, vol. 24, 2006, pp. 325-327.
[6] W. E. Dixon, D. M. Dawson, E. Zergeroglu, and A. Behal, “Adaptive Tracking Control of a Wheeled Mobile Robot via an Uncalibrated Camera System,” IEEE Tras. Systems, Man, amd Cybernetics, vol. 31, no. 3, June, 2001, pp. 341-352.
[7] H. Midorikawa, and K. Ohnishi, “A Proposal Sensor Fusion in Cooperative System,” 8th Int'l Workshop Advanced Motion Control, 2004, pp. 487-492.
[8] H. Y. Wand, S. Itani, T. Fukao, and N. Adachi, “Image-Based Visual Adaptive Tracking Control of Nonholonomic Mobile Robots,” Int'l Conf. Intelligent Robots and Systems, 2001, pp. 1-6.
[9] K. Hashimoto, and T. Noritsugu, “Visual Servoing of Nonholonomic Cart,” Int'l Conf. Robotics and Automation, 1997, pp. 1719-1724.
[10] Y. Ma, J. Kosecka, and S. Sastry, “Vision Guided Navigation for a Nonholonomic Mobile Robot,” IEEE Trans. Robotics and Automation, vol. 15, no. 3, 1999, pp. 521-536.
[11] H. Zhang, and J. P. Ostrowski, “Visual Motion Planning for Mobile Robots,” IEEE Trans. Robotics and Automation, vol. 18, no. 2, Apr. 2002, pp. 199-208.
[12] J. Chen, W. E. Dixon, D. M. Dawson, and M. McIntyre, “Homography-Based Visual Servo Tracking Control of a Wheeled Mobile Robot,” IEEE Trans. Robotics, vol. 22, no. 2, 2006, pp. 407-416.

김 곤 우

2000 중앙대학교 전자전기제어공학부(공학사)
2002 서울대학교 전기컴퓨터공학부(공학석사)
2006 서울대학교 전기컴퓨터공학부(공학박사)
2006~현재 한국생산기술연구원 선임연구원
관심분야 : Visual servoing, Robot Navigation, Sensor Fusion, Map Building and Localization

남 경 태

1995 영남대학교 전자공학과(공학사)
1997 영남대학교 전자공학과(공학석사)
2003~2006 고등기술연구소 선임연구원
2006~현재 한국생산기술연구원 선임연구원
관심분야 : 초정밀 모션제어, 무선 위치인식

이 상 무

1987 서울대학교 제어계측공학과(공학사)
1989 서울대학교 제어계측공학과(공학석사)
1999 서울대학교 전기공학부(공학박사)
1995~2000 고등기술연구원 책임연구원
2001~2004 (주)아이엠티 연구소장
2003~2005 고등기술연구원 수석연구원(겸직)
2003~현재 한국생산기술연구원 선임연구원
관심분야 : 초정밀로봇, 용접로봇, 자동화시스템 모션제어

손 웅 희

1988 서울산업대 기계설계학과(공학사)
1993 한양대학교 기계설계학과(공학석사)
1997 과학기술부 기계/차량기술사
1987~1990 한국과학기술원 기계공학과 연구원
1990~현재 한국생산기술연구원 수석연구원
관심분야 : 필드로봇, 생체역학, 수송기계